FAST CALCULATION OF THE SHIELDING EFFECTIVENESS FOR A RECTANGULAR ENCLOSURE OF FINITE WALL THICKNESS AND WITH NUMEROUS SMALL APERTURES

P. Dehkhoda, A. Tavakoli, and R. Moini

Electromagnetics Research Laboratory
Amirkabir University of Technology
15914, Hafez Ave., Tehran, Iran

Abstract—In this paper, an extremely fast technique is introduced to evaluate the shielding effectiveness of a rectangular enclosure of finite wall thickness and numerous square or circular small apertures subject to a normally incident plane wave. The technique is based on the traditional waveguide circuit model where the enclosure is replaced with an equivalent shorted transmission line. In the proposed circuit model, the perforated thick wall is represented by an equivalent impedance which is derived from the reflection coefficient. The computation results are in very good agreement with measurements. Additionally, further results are compared to a generalized modal MoM technique which are in excellent agreement as the number of apertures increase. Besides accuracy, the method is extremely efficient and easy to implement compared to the numerical techniques.

1. INTRODUCTION

Real electromagnetic shielding enclosures contain a large number of ventilating small apertures. Shielding effectiveness (SE) calculations of such metallic structures with small openings and large dimensions is complicated. There are many techniques that deal with multiple numbers of apertures in an enclosure. Approximate analytical methods are accurate but applicable only to simple geometries. A simple analytical method has been introduced by Robinson et al. based on a transmission line model [1]. In this method, the rectangular enclosure is modeled by a short-circuited rectangular waveguide and the aperture is represented by a coplanar strip transmission line. By neglecting the mutual coupling between multiple apertures, the perforated wall

impedance is the sum of the individual elements impedances. In [2], the mutual coupling between small holes and their lattice configuration are also taken into account. In addition to analytical techniques, a number of computational methods, such as transmission line modeling method-time Domain (TLM-TD) [3], the method of moments (MOM) and integral equations [4–7], finite element method (FEM) [8, 9] and finite difference time domain (FDTD) technique [10] have been proposed for the solution of shielding problems.

In the majority of the abovementioned methods, the effect of the perforated wall thickness is ignored to simplify the calculation. However, wall thickness has a significant impact on the SE of the perforated enclosure. At low frequencies, the thick aperture acts as a waveguide below cutoff and attenuates the field penetration through it. At high frequencies, due to the substantial electrical length of the aperture, the wall-aperture waveguide should be considered for accurate results. There are analytical approaches such as [11] in which the closed form expressions are derived for the equivalent magnetic current distributions over the apertures of filled grooves and slits in a thick infinite ground plane or [12] where the semi analytical MoM technique is utilized for several parallel thick plates with apertures. For the apertures in thick wall enclosures, numerical techniques such FDTD [13–15], transmission line matrix (TLM) [16, 17] and mode matching [18] can deal with the wall thickness, but at the cost of solution complexity and CPU time. The robustness of the numerical techniques is severely limited by the size of the aperture and its thickness relative to the cavity dimensions.

In this paper, the original waveguide equivalent circuit model of [1] is modified to take into account the wall thickness of the perforated wall with a large number of square or circular apertures. It can be shown that although the aperture thickness is considered in [1] to yield an equivalent impedance for the represented coplanar strip transmission line, it does not confirm the real effect of the aperture thickness on the SE, specially for the large thicknesses. Here, the perforated thick wall is represented by its reflection coefficient reported in [19] between free space and the enclosure. Then, similar to [1], the enclosure is modeled as a shorted waveguide represented by its equivalent transmission line model. Here, a TE_{10} propagating mode is assumed and the incident wave is modeled by a voltage source and the free-space impedance in the equivalent circuit. As reported in [2], since the mutual coupling between the openings and the lattice arrangement are taken into account in the admittance of the wall, the results are more accurate than that of the traditional circuit model of [1]. The theoretical results are in a very good agreement with the measurements reported in [16]

for an array of small circular holes. For square apertures, the SE of this model is compared with the generalized modal method of moments (GMMoM) technique results. The agreement between the results increases as the number of apertures augments. Since this technique considers the effect of wall thickness in the analysis, it is more accurate when compared to methods that ignore the thickness. In addition, this technique is extremely time efficient for enclosures with a large number of apertures where alternative full wave numerical solutions are very time consuming. As in [2], just the dominant TE_{10} mode is considered here for the equivalent waveguide. The restrictions of the presented transmission line model such as normally incident plane wave, central apertures and observation points along with the limitation on the frequency range can be overcome considering [20–22]. This method is applicable to square and equilateral lattice arrangements of holes of square and circular shapes.

2. EQUIVALENT TRANSMISSION LINE MODEL

2.1. Impedance of an Array of Small Holes in a Finite-Thickness Plate

Figure 1 shows an infinite metallic flat plate of finite thickness with square and circular holes in a square lattice. For normal incidence, the reflection coefficient of a reflector screen can be reduced to

$$R = \frac{1}{1 - j\left[A + B\tanh(\beta t/2)\right]} + \frac{1}{1 - j\left[A + B\coth(\beta t/2)\right]} - 1, \quad (1)$$

where t is the perforation thickness; A and B are functions of element spacing, aperture size, and wavelength, and β is the propagation constant of the field inside the holes [19]. In addition to a square lattice configuration, the apertures could be distributed in an equilateral triangular lattice structure whose A and B are also reported in [19].

Equation (1) is valid below the aperture cut-off frequency where only the dominant waveguide mode is significantly present in the openings. The aperture size and spacing between them should meet the conditions in Table 1.

The equivalent impedance of the array of apertures is $Z_{ah} = \eta_0 \frac{1+R}{1-R}$, where η_0 is the free space intrinsic impedance. For an enclosure wall with its center partially perforated by an array of holes, the effective wall impedance Z'_{ah} is a fraction of Z_{ah}. Using an impedance ratio concept Z'_{ah} becomes [2]

$$Z'_{ah} = \alpha Z_{ah}, \quad (2)$$

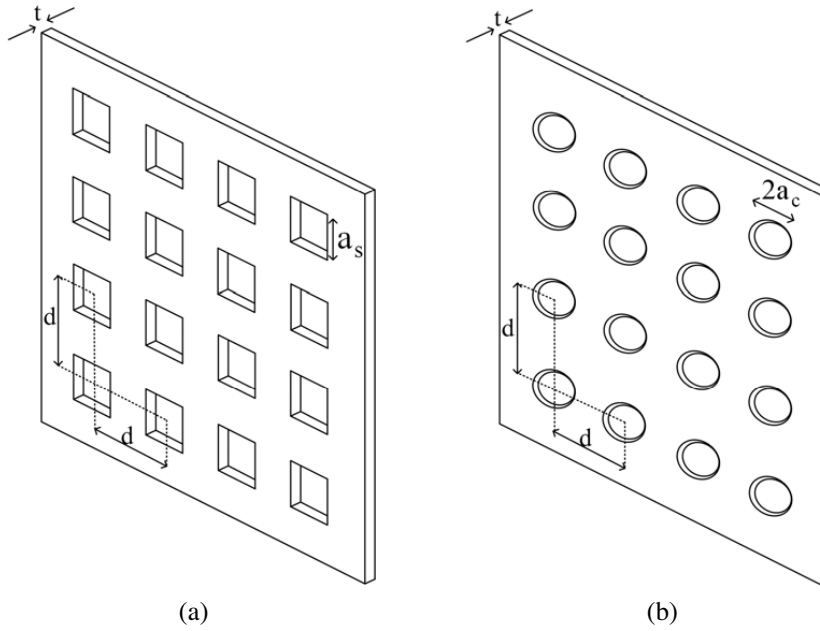(a)   (b)

Figure 1. Geometry of an array of holes in a metallic flat plate in square lattice; (a) square and (b) circular apertures.

Table 1. Shape, size and spacing of the holes for different lattice configurations.

Shape of openings	Type of lattice configuration	Openings size	Element separation
Circular	Equilateral	$a_c > 0.28d$	$d < 0.57\lambda$
Circular	Square	$a_c > 0.28d$	$d < 0.5\lambda$
Square	Equilateral	$a_s > 0.5d$	$d < 0.57\lambda$
Square	Square	$a_s > 0.5d$	$d < 0.5\lambda$

where α is the ratio of the perforated area to the whole surface. Here, the traditional circuit model is improved by this proper choice of aperture impedance that considers the finite wall thickness, the hole lattice arrangement, and the mutual coupling between them.

2.2. Equivalent Circuit Model

Figure 2 shows a rectangular perfect electric conductor enclosure of finite wall thickness with an array of holes exposed to an incident plane wave and the equivalent circuit model of the structure. The enclosure is modeled as a shorted waveguide whose characteristic impedance and propagation constant are Z_g and k_g, respectively [1]. For the TE$_{10}$ mode of propagation in the enclosure, $Z_g = \eta_0/\sqrt{1 - (\lambda_0/2a)^2}$ and $k_g = k_0\sqrt{1 - (\lambda_0/2a)^2}$, where k_0 and λ_0 are the free space propagation constant and wavelength, respectively. The incident wave is represented by the voltage V_0 and the free space intrinsic impedance $\eta_0 \approx 377\,\Omega$. The impedance Z'_{ah} represents the array of small holes in the finite-thickness wall linking free space with the waveguide.
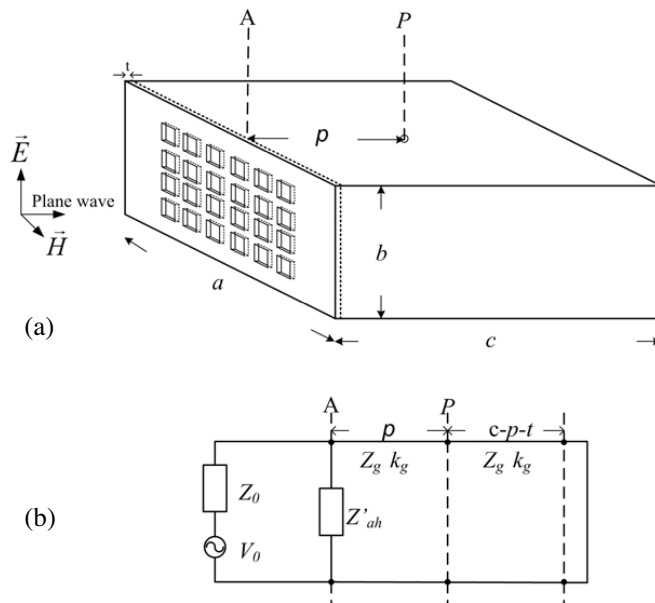

Figure 2. A rectangular box with an array of holes (a) exposed to an incident plane wave and (b) its equivalent circuit model.

2.3. Electric and Magnetic Shielding Effectiveness

The electric and the magnetic SE at point P at distance p from the perforated wall is obtained from the voltage and current at that point in the equivalent circuit of Fig. 2. The details of the derivation and the resultant formulas for SE are given in [1].

3. GENERALIZED MODAL MOM TECHNIQUE

The modal MoM technique in [23] can be generalized to include the wall thickness in a SE calculation of a perfect electric conductor box with rectangular apertures [24]. It is assumed that apertures are small enough so that image theory can be applied. Additionally, the edge diffracted fields are ignored. Here, in the generalized approach, by using the surface equivalence principle, each aperture is replaced by two sets of equivalent magnetic currents at both sides. The problem is divided into three separate regions of outside the enclosure, inside the aperture, and inside the enclosure. Fig. 3 depicts the side view of the enclosure and its rth aperture, where Fig. 3(a) shows the aperture fields and 3(b) represents their equivalent magnetic currents, respectively.
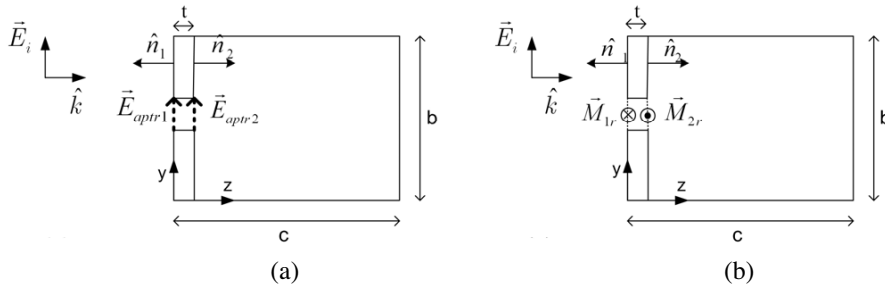

Figure 3. Enclosure side view with (a) electric fields and (b) equivalent magnetic currents at both sides of the aperture.

The rectangular configuration of the enclosure and the apertures allows the use of sinusoidal modal expansions for the transverse electrical fields. Then, using the equivalence principle, the equivalent magnetic currents at each side of the rth aperture are:

$$\vec{M}_{1r} = \hat{n}_1 \times \vec{E}_{aptr1} = \sum_{r=1}^{R} \left[\hat{x} \sum_p \sum_q U_{rpq} \Psi_r - \hat{y} \sum_p \sum_q V_{rpq} \Phi_r \right], \quad (3)$$

$$\vec{M}_{2r} = \hat{n}_2 \times \vec{E}_{aptr2} = \sum_{r=1}^{R} \left[-\hat{x} \sum_p \sum_q A_{rpq} \Psi_r + \hat{y} \sum_p \sum_q B_{rpq} \Phi_r \right], (4)$$

where U_{rpq} and V_{rpq} are the unknown amplitudes of the pqth mode of the magnetic current on the outer face of the enclosure which are nonzero at the rth aperture and zero elsewhere. Similarly, A_{rpq} and B_{rpq} are defined for the inner face of the enclosure. In addition, R indicates the number of apertures, L_r and W_r are the length and width

of the rth aperture, x_{cr} and y_{cr} are its center coordinates, and

$$\Psi_{rpq} = \sin\left(\frac{p\pi}{L_r}(L_r/2 + x - x_{cr})\right)\cos\left(\frac{q\pi}{W_r}(W_r/2 + y - y_{cr})\right), (5)$$

$$\Phi_{rpq} = \cos\left(\frac{p\pi}{L_r}(L_r/2 + x - x_{cr})\right)\sin\left(\frac{q\pi}{W_r}(W_r/2 + y - y_{cr})\right). (6)$$

In Fig. 4(a), Region I is the outer area and is assumed to be a half free space. The total field in this region is the sum of the radiated fields from $\vec{M}_{1r}$, the incident wave, and its reflection. Region II is the volume composed of the aperture sides and the thick wall as shown in Fig. 4(b). The total field in this region is the sum of radiated fields from $-\vec{M}_{1r}$ and $-\vec{M}_{2r}$.
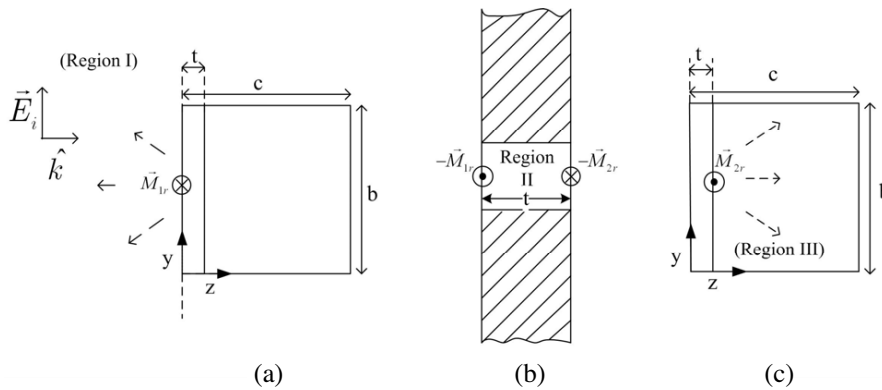

Figure 4. Division of the problem space into (a) Region I, outside the enclosure, (b) Region II, within the wall, and (c) Region III, inside the enclosure.

The negative currents satisfy the continuity of the tangential electric field on both sides of the aperture. Inside the enclosure is the third region where the total field is just radiated from $\vec{M}_{2r}$. Electromagnetic fields in terms of the electric vector potential $\left(\vec{F}\right)$ are given as:

$$\vec{E} = \sum_{r=1}^{R}\left(-\frac{1}{\varepsilon_0}\nabla \times \vec{F}\right), \tag{7}$$

$$\vec{H} = \sum_{r=1}^{R}\left(\frac{-j\omega}{k_0^2}\left(k_0^2\vec{F} + \nabla\nabla \cdot \vec{F}\right)\right), \tag{8}$$

where $\vec{F}$ is defined as:

$$\vec{F}_r = \iint\limits_{aperture} \int \tilde{G}_m(x,y,z/x',y',z') \cdot \vec{M}_r(x',y',z')dx'dy'dz', \quad (9)$$

and $\tilde{G}_m(x,y,z/x',y',z')$ is the Green's function of each region [24]. By enforcing the tangential magnetic field boundary condition at each side of an aperture, two sets of integral equations for the magnetic currents of each aperture are derived. Then, the Galerkin MoM approach solution is used to find the electromagnetic fields in all space.

4. COMPARISON WITH MEASUREMENTS AND THE GMMOM TECHNIQUE

4.1. Comparison with Measurements

An empty $36 \times 12 \times 42$ cm rectangular enclosure with holes, as shown in Fig. 5, is analyzed with our modified waveguide equivalent circuit model. The wall thickness is $t = 1.2$ mm, and the radius of the circular holes and their separation are $a_c = 5$ mm and $d = 12$ mm, respectively. Electrical SE is computed at the point P, in the mid plane parallel to the side walls, 4 cm from the back wall and 2 cm from the enclosure lid.
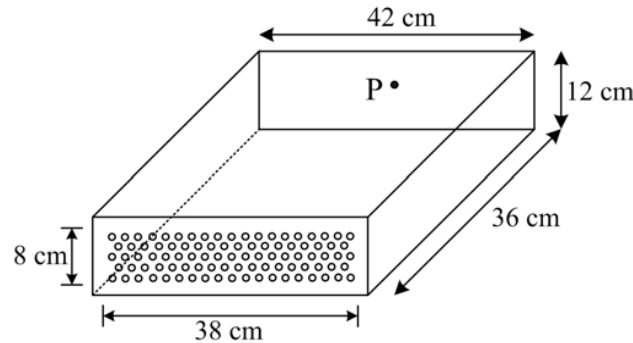

Figure 5. An enclosure with equilateral lattice structure of circular holes.

The y-polarized normally incident plane wave allows the use of the proposed circuit model to find the SE at point P. Fig. 6 depicts the SE from this model, measurements [16] and the TLM [16]. As illustrated, the results of this method are in better agreement with measurements than TLM predictions. Since the proposed technique deals only with a

simple circuit analysis, it is more efficient than the TLM technique that discretizes the space of the problem and uses an iterative approach at each cell to obtain voltages and currents and thus the final result. Our equivalent circuit model requires less than 0.05 milliseconds of CPU time on a 2.68 GHz computer at each frequency, thus, it is not only very simple to implement but also computationally extremely fast.
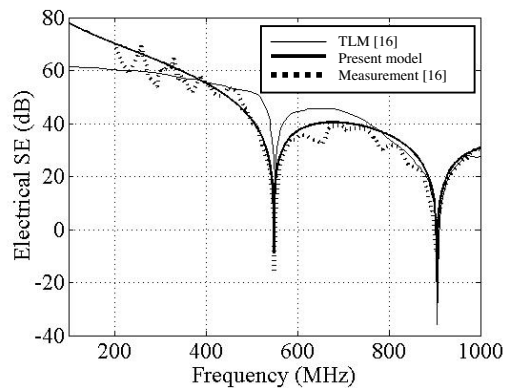

Figure 6. Comparison between the electrical SE of the present model and the measurements of [16] for the enclosure of Fig. 5.

The resonant frequencies of the box without apertures up to 1 GHz are 357.1, 548.8, 714.3, 826.9 and 906.6 MHz. As observed in Fig. 6 since the apertures' size are very small compared to the enclosure dimension, the perforation in the enclosure does not change the resonant frequencies and two resonant frequencies of 548.8 and 906.6 MHz appear in the figure. The other resonances are omitted due to symmetry. It should be noted that in all the examined cases in this paper the array of holes is are located at the centre of the front face.

4.2. Comparison with the GMMoM

Further validation is performed by comparing the results of the newly proposed circuit technique with the GMMoM [24]. A 50 cm cubic enclosure with various numbers of 4 cm square apertures and 5 mm thickness is examined. The holes are distributed in a square lattice of 6 cm separation. Fig. 7 shows the SE of the circuit model and GMMoM at the centre of the enclosure. As the number of apertures increases, the two approaches are in better agreement, while the calculation time of the numerical method increases remarkably that is validated in Table 2. Since the reflection coefficient in (1) is derived for an infinite plate completely covered by the apertures, the model becomes

Table 2. Comparison of the CPU time.

aperture array	CPU time for each frequency analysis	
	GMMoM	Present Circuit Model
4 x 4	4.36 minute	<0.05 ms
6 x 6	19.51 minute	<0.05 ms
8 x 8	57.71 minute	<0.05 ms

Table 3. SE of the enclosure in Fig. 7(c) for different thicknesses.

Thickness (cm)	SE (dB)			
	Frequency 200 MHz		Frequency 500 MHz	
	Present Circuit Model	GMMoM	Present Circuit Model	GMMoM
0.1	40.50	38.97	21.55	20.02
0.5	41.88	42.07	22.90	22.09
0.7	42.32	43.54	23.33	24.55
0.9	42.64	44.98	23.66	25.98
2	43.40	52.64	24.40	33.59

more accurate as the total surface area of perforations increase. Again here the presence of the small apertures does not alter the resonant frequency of the enclosure.

4.3. Effect of the Wall Thickness on the SE

Table 3 compares the SE of this method and GMMoM for the configuration of Fig. 7(c) at 200 and 500 MHz for various wall thicknesses. As shown, by increasing the wall thickness a higher SE is achieved. However, as the thickness increases beyond 0.7 cm, the agreement between the two methods diminishes.

In order to study the effect of wall thickness on small apertures, the SE at the central point of a $30 \times 12 \times 30$ cm enclosure with 20 circular holes and various thicknesses is shown in Fig. 8. The holes of 6 mm radius are distributed in an equilateral configuration of 20 mm separation distance (Fig. 8). As shown, the SE improves as the wall thickness increases. Please note that there is a 3 dB difference between the SE of $t = 0.0001$ mm (approximately zero thickness) and $t = 2$ mm, which means that wall thickness should be considered for accurate SE prediction particularly for small apertures. Such a behavior is also observed for square thin holes.
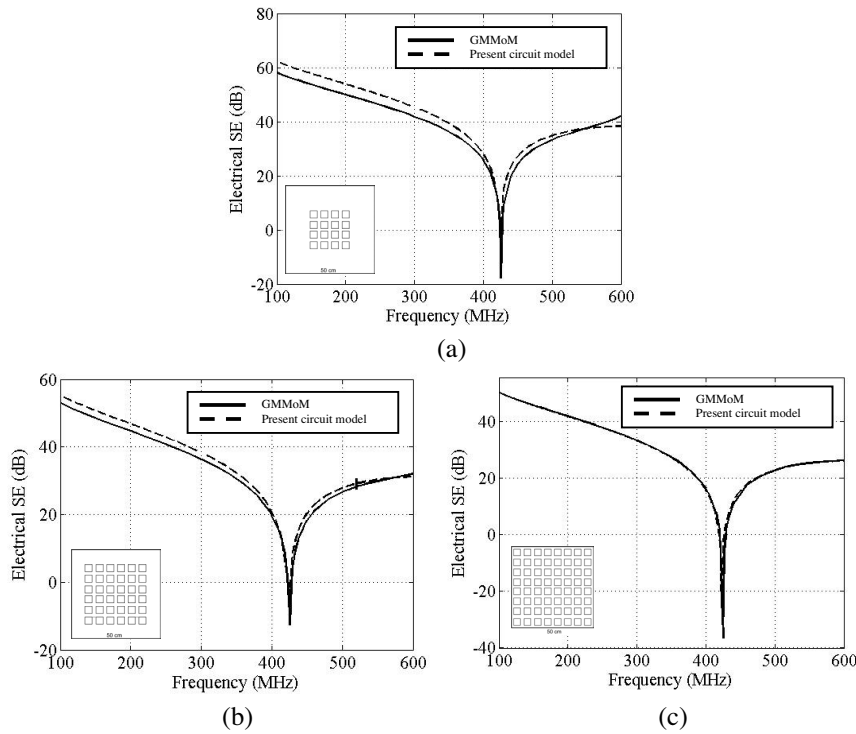
Figure 7. Comparison between the electrical SE of the present model and the GMMoM of [24] for a cubic enclosure of 50 cm with 4 cm square holes of 6 cm separation for (a) 4×4, (b) 6×6, and (c) 10×10 element aperture array.

4.4. Validation in the Limiting Case of Zero Thickness

For the case of zero thickness, the method is compared with the circuit model of [2] where a proper impedance is used for circular perforations with equilateral and square configurations. A $30 \times 12 \times 30$ cm enclosure with circular openings of 7.5 mm radius and separation of 17.5 mm with two square and equilateral arrangements is studied. As shown in Fig. 9, the results of the two approaches for the central point of the enclosure are identical.

4.5. Discussion on the Thickness of the Wall

As the thickness of the wall increases, the argument of the hyperbolic tangent function in (1) tends towards 1. Therefore, the validity of
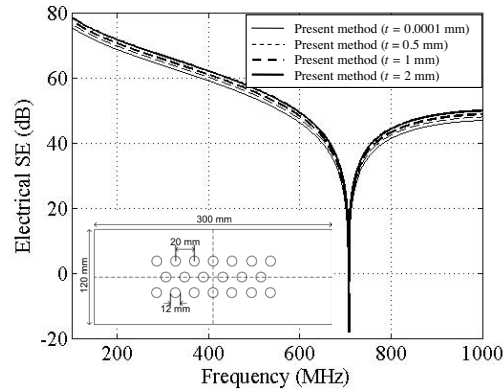
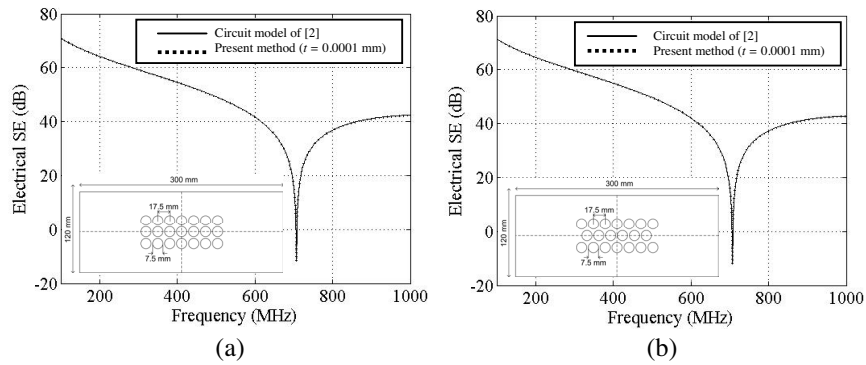**Figure 8.** Effect of various wall thicknesses on SE.

Figure 9. Comparison between the electrical SE of the present model for infinitesimally small thickness wall and the model in [2] for the circular holes of (a) square and (b) equilateral lattice structure.

the circuit model is limited to thicknesses whose $\beta t/2$ remains in the linear region of the hyperbolic tangent function; thus, $\beta t/2 < 0.4$ is a good approximation for this criterion. Fig. 10 compares the SE at the central point of a $50\,\mathrm{cm}$ cubic enclosure with 6×6 square holes of $2\,\mathrm{cm}$ and separation of $3.5\,\mathrm{cm}$ for various wall thicknesses. As shown for $t > 5\,\mathrm{mm}$ where the hyperbolic tangent is not linear, the calculated SE is incorrect. Disagreement between two calculated SE for $t > 0.7\,\mathrm{cm}$ in Table 3 confirms this fact.
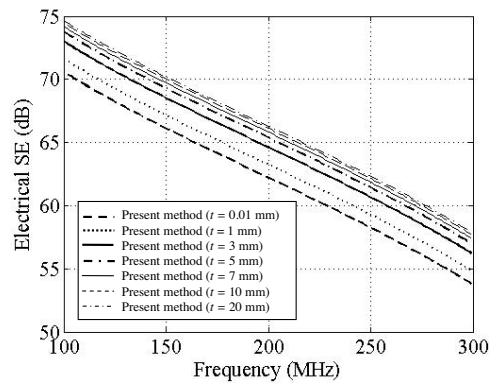
Figure 10. Effect of increasing wall thickness on calculated SE.

5. CONCLUSION

In this paper, an enclosure with numerous apertures in a finite thickness wall is modeled by a very efficient analytical approach based on waveguide equivalent circuit model. The model supports the square and circular openings with square and equilateral lattice structures. The impedance used for the perforated wall takes the mutual coupling between the apertures into account consistent with their lattice configuration in the thick wall. This highly efficient and simple to implement method is proved to be very accurate when compared to measurements and the GMMoM technique. It is shown that wall thickness has a noticeable effect on SE particularly for small apertures and thus, it should be considered in SE calculations.

REFERENCES

1. Robinson, M. P., T. M. Benson, C. Christopoulos, J. F. Dawson, M. D. Ganley, A. C. Marvin, S. J. Porter, and D. W. P. Thomas, "Analytical formulation for the shielding effectiveness of enclosures with apertures," *IEEE Trans. Electromagn. Compat.*, Vol. 40, No. 3, 240–248, Aug. 1998.
2. Dehkhoda, P., A. Tavakoli, and R. Moini, "An efficient and reliable shielding effectiveness evaluation of a rectangular enclosure with numerous apertures," *IEEE Trans. Electromag. Compat.*, Vol. 50, No. 1, 208–212, Feb. 2008.
3. Bahadorzadeh, M. and M. N. Moghaddasi, "Improving the shielding effectiveness of a rectangular metallic enclosure

with aperture by using extra shielding wall," *Progress In Electromagnetics Research Letters*, Vol. 1, 45–50, 2008.

4. Yla-Oijala, P., M. Taskinen, and J. Sarvas, "Surface integral equation method for general composite metallic and dielectric structures with junctions," *Progress In Electromagnetics Research*, PIER 52, 81–108, 2005.

5. Matsushima, A., Y. Nakamura, and S. Tomino, "Application of integral equation method to metal-plate lens structures," *Progress In Electromagnetics Research*, PIER 54, 245–262, 2005.

6. Nie, X. C. and N. Yuan, "Accurate modeling of monopole antennas in shielded enclosures with apertures," *Progress In Electromagnetics Research*, PIER 79, 251–262, 2008.

7. Wei, X. C., E. P. Li, and C. H. Liang, "Fast solution for large scale electromagnetic scattering problems using wavelet transform and its precondition," *Progress In Electromagnetics Research*, PIER 38, 253–267, 2002.

8. Edrisi, M. and A. Khodabakhshian, "Simple methodology for electric and magnetic shielding effectiveness computation of enclosures for electromagnetic compatibility use," *Journal of Electromagnetic Waves and Applications*, Vol. 20, No. 8, 1051–1060, 2006.

9. Ojeda, X. and L. Pichon, "Combining the finite element method and Pade approximation for scattering analysis application to radiated electromagnetic compatibility problems," *Journal of Electromagnetic Waves and Applications*, Vol. 19, No. 10, 1375–1390, 2005.

10. Lei, J. Z., C. H. Liang, and Y. Zhang, "Study on shielding effectiveness of metallic cavities with apertures by combining parallel FDTD method with windowing technique," *Progress In Electromagnetics Research*, PIER 74, 82–112, 2007.

11. Barkeshli, K. and J. L. Volakis, "Scattering from narrow grooves and slits," *Journal of Electromagnetic Waves and Applications*, Vol. 6, Nos. 1–4, 459–474, 1992.

12. Robertson, J., E. A. Parker, B. Sanz-Izquierdo, and J. C. Batchelor, "Electromagnetic coupling through arbitrary apertures in parallel conducting planes," *Progress In Electromagnetics Research B*, Vol. 8, 29–42, 2008.

13. Jiao, C., X. Cui, L. Li, and H. Li, "Subcell FDTD analysis of shielding effectiveness of a thin-walled enclosure with an aperture," *IEEE Trans. Magnetics*, Vol. 42, No. 4, 1075–1078, Apr. 2006.

14. Edelvik, F. and T. Weiland, "Stable modeling of arbitrarily oriented thin slots in the FDTD method," *IEEE Trans. Electromag. Compat.*, Vol. 47, No. 3, 440–446, Aug. 2005.

15. Wang, J. and W. J. Koh, "Electromagnetic coupling analysis of transient signal through slots or apertures perforated in a shielding metallic enclosure using FDTD methodology," *Progress In Electromagnetics Research*, PIER 36, 247–264, 2002.

16. Paul, J., V. Podlozny, and C. Christopoulos, "The use of digital filtering techniques for the simulation of fine features in EMC problems solved in the time domain," *IEEE Trans. Electromag. Compat.*, Vol. 45, No. 2, 238–244, May 2003.

17. Podlozny, V., C. Christopoulos, and J. Paul, "Efficient description of fine features using digital filters in time-domain computational electromagnetics," *IEE Proceedings — Science, Measurement and Technology*, Vol. 149, No. 5, 254–257, Sept. 2002.

18. Park, H. H. and H. J. Eom, "Electromagnetic penetration into a rectangular cavity with multiple rectangular apertures in a conducting plane," *IEEE Trans. Electromag. Compat.*, Vol. 42, No. 3, 303–307, Aug. 2000.

19. Chen, C. C., "Transmission of microwave through perforated flat plates of finite thickness," *IEEE Trans. Microwave. Theory Tech.*, Vol. 21, No. 1, 1–6, Jan. 1973.

20. Belokour, I., J. LoVetri, and S. Kashyap, "A higher-order mode transmission line model of the shielding effectiveness of enclosures with apertures," *IEEE Int. Symp. Electromag. Compat.*, 702–707, Aug. 13–17, 2001.

21. Shim, J. J., D. G. Kam, J. H. Kwon, H. D. Choi, and J. Kim, "Circuital approach to evaluate shielding effectiveness of rectangular enclosures with apertures on multiple sides," *EMC Europe 2004, Int. Symp. Electromag. Compat.*, Eindhoven, The Netherlands, Sept. 6–10, 2004.

22. Dan, S., S. Yuanmao, and Y. Gao, "3 high-order mode transmission line model of enclosure with off-center aperture," *IEEE Int. Symp. Electromag. Compat.*, 361–364, 2007.

23. http://techreports.larc.nasa.gov/ltrs/PDF/2000/cr/NASA-2000-cr210 297.pdf, accessed July 2006.

24. Dehkhoda, P., A. Tavakoli, and R. Moini, "Shielding effectiveness of a rectangular enclosure with finite wall thickness and rectangular apertures by the generalized modal MoM," accepted to be published in *IET Science, Measurement and Technology*.